

Time-Resolved Charge Transfer in “Push-Pull” Stilbenes

Jean Oberlé, Gediminas Jonusauskas, Emmanuel Abraham, René Lapouyade[†], and Claude Rullière*

Centre de Physique Moléculaire Optique et Hertzienne, UMR CNRS n°5798, Université Bordeaux I,
351 Cours de la Libération, 33405 Talence, France

[†]Laboratoire d'Analyse Chimique par Reconnaissance Moléculaire (LACReM), Université Bordeaux I,
351 Cours de la Libération, 33405 Talence, France

(Received September 25, 2001)

Intramolecular Charge Transfer (ICT) processes of 4-dimethylamino-4'-nitrostilbene (DNS) in solution are studied by pump-probe absorption spectroscopy with a 100 fs time resolution. The results are compared to transient CARS experiments. Pump-probe results confirm the formation of a radiative ICT state in low polar solvents. In a highly polar solvent (acetonitrile), the formation of a short-lived non-radiative ICT state is observed for the first time. CARS experiments support structural changes associated to ICT processes in highly polar solvents.

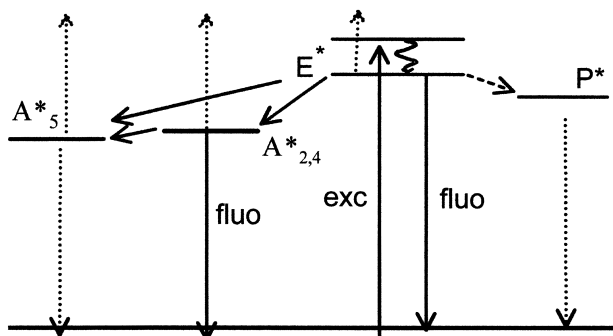
Photoinduced intramolecular charge transfer (ICT) processes in donor–acceptor substituted stilbenes have been the subject of many theoretical and experimental investigations over the past years. ICT processes are known to be strongly dependent on solvent–solute interactions and the existence of twisted or “conformational relaxed” ICT states have been proposed.^{1–5} Among others, the existence of ICT states in 4-dimethylamino-4'-cyanostilbene (DCS) has attracted much attention and the photophysics of DCS has been studied by time-resolved fluorescence up-conversion, pump-probe and Kerr ellipsometry experiments.^{3–8}

For this compound, it has been proposed that, just after excitation and on a sub-picosecond time scale, the initial excited state transforms into an intramolecular charge transfer state (E^*) without any deviation from the initial conformation (see Scheme 1). In polar solvents, in addition to the stilbene-type “phantom-singlet” state (P^*) formed by double bond twisting, a highly polar and fluorescent conformational relaxed ICT (CRICT) state (the so called $A^*_{2,4}$ state in⁵), is then formed from the (E^*) state by single bond twisting involving the rotation of the dimethyl-anilino group (see Scheme 1). Since in

polar solvents the P^* state is less polar than the ICT state, the energy barrier $ICT \rightarrow P^*$ increases and the isomerization route is strongly quenched by the transition from the ICT state to the conformational relaxed ICT state.^{3–8}

Although the photophysics of DCS has been studied in detail, information about the similar 4-dimethylamino-4'-nitrostilbene (DNS) molecule remains limited. However, this molecule is interesting because of the NO_2 group which should strongly enhance the charge transfer process and therefore highlight the role of ICT. Compared to DCS, the peculiar fluorescence behavior of DNS, i.e. the fluorescence quantum yield increases from weakly polar solvents to moderately polar solvents and then decreases in highly polar solvents, has been explained from steady state measurements by the presence (see Scheme 1) of a further ICT state (A^*_5) in addition to the $A^*_{2,4}$ CRICT state.⁵ This A^*_5 state, considered as a TICT state⁵, involves the rotation of the nitro group. In non-polar (or moderately polar) solvents, the energy of the $A^*_{2,4}$ state is presumably lower than the energy of the A^*_5 state and is therefore populated preferentially, leading to a high fluorescence quantum yield. However, in polar solvents, the branching ratio of E^* to $A^*_{2,4}$ and A^*_5 states is changed by the solvent–solute interaction which leads to a lowering of the energy of the highly polar and non-radiative A^*_5 state. In strongly polar solvents, the A^*_5 state is therefore populated preferentially, causing a dramatic decrease of the fluorescence quantum yield of DNS.^{5,9,10,11}

When investigating charge transfer processes, Hamaguchi et al.¹² recently observed a $\sim 120\text{ cm}^{-1}$ downshift in polar solvents for the $C\equiv N$ stretch wavenumber after excitation of the DMABN molecule, the accepted model for TICT state studies. This is the first time an experiment showed the role of the rotation of the cyano group during the charge transfer state formation, which supports the hypothesis of a structural change associated to ICT state formations in this compound. As to the DNS molecule, Raman and infrared absorption spectra of unexcited and excited DNS in polar solvents revealed a 39 cm^{-1}



Scheme 1. Description of the involved energy levels in the push-pull stilbenes. Fluo: fluorescence. Exc: Excitation. Dashed lines: non-radiative transitions.

downshift of the NO₂ symmetric stretch wavenumber in the excited state, in agreement with the existence of an A₅^{*} state stabilized by the rotation of the nitro group in highly polar solvents.¹³ Nevertheless, the 60 ps time resolution of these experiments was unable to time-resolve the formation and relaxation of the A₅^{*} state and no data were obtained in weakly polar solvents in which this state is not supposed to be populated. Recently, picosecond time-resolved CARS experiments have revealed different vibrational behaviors in DNS between strongly and moderately polar solvents, indicating the possible formation of two different ICT states.¹⁴ Particularly a downshift of the NO₂ stretching mode in a strongly polar solvent (acetonitrile) is in good agreement with the formation of the so-called A₅^{*} state since this downshift is not observed in toluene for example.

In this paper, we take advantage of the 100 fs time resolution which can be obtained with pump-probe experiments to present new results concerning DNS photophysics. These results are analyzed taking into account previous results obtained by CARS experiments¹⁴ and lead to more detailed information about the photophysics of DNS in low and highly polar solvents.

Experimental

Materials 4-Dimethylamino-4'-nitrostilbene (DNS) was synthesized according to Refs. 5 and 15 and dissolved in solvents of spectroscopic grade (Aldrich). For the pump-probe experiments, the DNS solutions (concentrations $\sim 10^{-3}$ M) were contained in flowing optical quartz cells of 2 mm path length. For the CARS experiments, we used a free flowing jet (~ 300 μ m thickness) with concentrations of about 10^{-3} M in toluene and 4×10^{-3} M in acetonitrile.

"Pump-Probe" Experiment The pump-probe experiment is based on a self-mode-locked Cr⁴⁺:Forsterite oscillator generating 30 fs pulses at 1200 nm followed by a stretcher-amplifier-compressor stage, previously described in detail.¹⁶ The laser system routinely generated pulses of ~ 120 fs centered around 1200 nm (100 μ J, 1 kHz repetition rate). As shown in Fig. 1, the laser pulses are split in two parts, producing the pump and the probe pulses respectively. The pump pulse (400 nm, ~ 5 μ J) is generated after frequency tripling by a third harmonic generator formed by a 1 mm BBO crystal and a 1 mm KDP crystal. The probe is a white light continuum pulse, extending from $\omega_c = 350$ nm to 1000 nm, generated by focusing the second part of the pulses (~ 3 μ J per pulse) with a 150-mm lens into a 10 mm thick D₂O flow cuvette. In order to minimize the shot-to-shot fluctuation, part of the probe pulse is split off for reference before interaction with the sample and is directed into the spectrograph by means of an optical fiber. The remaining part of the continuum is used as a probe pulse to monitor the transient absorption spectra of the sample at different time delays Δt between the pump pulse and the continuum probe pulse. The pump and the probe beam are focused into the sample by a 15 cm focal-length, and to ensure rotational reorientation effect-free kinetics, the angle between the linearly polarized pump and probe beams is set to the magic angle 54.7°. The detection system was a spectrograph (Chromex 5001 S) coupled to a CCD camera (Sony XC-ST50) connected to a computer for spectrum data analysis. The probe pulse and the reference pulse are focused separately into the spectrograph to form two spectrally resolved images on the CCD camera and are recorded by accumulating

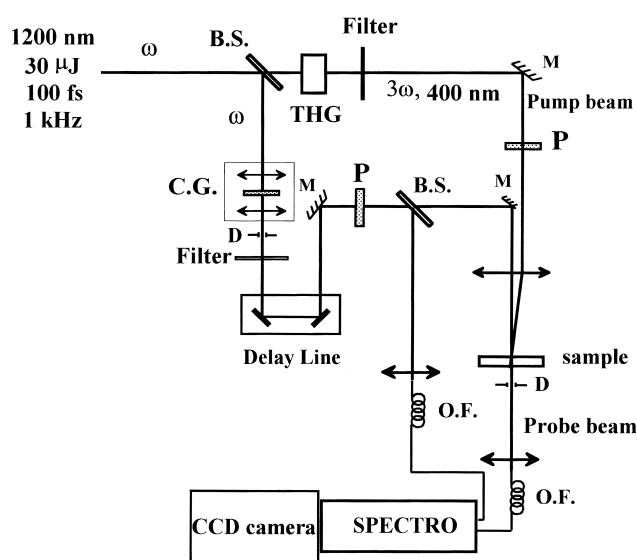


Fig. 1. Experimental setup. BS: beam splitter, THG: third harmonic generator, C.G: continuum generator, M: mirror, P: polarizer, D: pin-hole, O.F.: optical fiber.

2000 laser shots. The time dispersion of the white-light continuum probe pulse was corrected by determining the dispersion of the temporal zero-position $\Delta t(v_i) = 0$ from the transient Kerr signal of a 300 μ m thick CS₂ cell at spectra intervals of about 1 nm corresponding to the spectral resolution of the detection system. Therefore, spectral distributions of the continuum corrected for background signal, shot-to-shot fluctuation and time dispersion, in presence and in absence of the pump pulse at different time delays between the pump and the probe pulses, determined the transient absorption on a 100 femtosecond time-scale with an error of about 0.005 for the optical density.

CARS Technique and Experimental Set-Up Since at the end of this paper, we will compare "pump-probe" results to time-resolved CARS experiments, we would like to recall the experimental conditions in which these results have been obtained. In the time-resolved degenerate (two-colors) polarization sensitive CARS technique, three pulses are required to generate the CARS signal from an excited sample: one pulse (the "pump pulse") at a fixed frequency ω_1 and the second pulse (the "Stokes pulse") at a variable frequency ω_2 such that $\omega_1 - \omega_2 = \Omega$, the molecular vibration frequency to be observed. The CARS signal is then generated at frequency $\omega_{\text{cars}} = 2\omega_1 - \omega_2$ in a well-defined propagation direction determined by the phase matching conditions. Finally, the third beam at frequency ω_{exc} is used to create the excited population. Before presenting the experimental set-up, a brief reminder of a few specific properties of CARS spectra is required here.

The CARS signal of a molecular species in solution, excited to the S₁ electronic state, is proportional to the squared modulus of the third-order nonlinear optical susceptibility and can be expressed as:¹⁷

$$I_{\text{CARS}} \propto |\chi^{(3)}|^2 = |\chi_{\text{solv}}^{\text{NR}(3)} + \sum \chi_{\text{solv}}^{\text{R}(3)} + \sum \chi_{\text{S}_0}^{\text{R}(3)} + \sum \chi_{\text{S}_{\text{exc}}}^{\text{E}(3)} + \sum \chi_{\text{S}_{\text{exc}}}^{\text{R}(3)}|^2 \quad (1)$$

The first two terms are respectively the non-resonant susceptibility and the Raman resonance susceptibility of the solvent. The third term is associated with Raman resonances of the ground

state while the last two terms are the pure electronic susceptibility and the Raman resonance susceptibility of the excited states. These different contributions to the CARS spectra may change as a function of time during the relaxation processes. The non-resonant contributions affect the spectral shape of the CARS spectra and make the analysis of CARS spectra difficult. However it is possible to suppress the non-resonant part of the CARS signal by adjusting the polarizations of the pump (ω_1) and of the Stokes (ω_2) pulses as well as the orientation angle of the analyzer with respect to these two pulses.^{17–20} In these conditions, the CARS bands show a Lorentzian shape, the signature of a vibrational mode of the solution (solvent, ground state or excited states). For the vibrational modes of excited DNS, the square root of the intensities of these bands are proportional to the excited state populations since $\chi^{(3)} \propto N \cdot \gamma^{(3)}$, where N is the density of the excited molecular species and $\gamma^{(3)}$ the molecular hyperpolarisability.

The time-resolved degenerate (two-colors) polarization sensitive CARS apparatus, described in detail elsewhere,²¹ is based on a hybrid mode-locked dye laser associated with an actively mode-locked cw-pumped Nd:YAG laser, a dye amplifier and a Nd:YAG regenerative amplifier. The laser system generates pulses of ~ 1 ps (1 mJ, 10 Hz repetition rate) tuned around 600 nm. The different optical beams are obtained after splitting the output beam of the laser system into three parts. The first part is used as the ω_1 pump beam (at 600 nm) for the generation of the CARS signal. The second part is focused into a 2 cm water cell to produce a 2 ps light continuum (extending from ~ 350 to ~ 900 nm). The Stokes beam at variable frequency ω_2 is obtained from the continuum after selecting a spectral bandwidth of 2000 cm^{-1} centered at 640 nm and amplified (up to $100\text{ }\mu\text{J/pulse}$) by a two stages dye amplifier (DCM) pumped by the frequency doubled output of the regenerative amplifier (532 nm, 70 ps, 10 Hz). Thus the CARS spectrum of the sample could be obtained over a wide spectral range (frequency $\omega_1 - \omega_2 = \Omega$ from 800 to 2500 cm^{-1}). Finally, the third part at 600 nm is frequency doubled in a KDP crystal ($\omega_{\text{exc}} = 300\text{ nm}$, ~ 1 ps and $10\text{--}50\text{ }\mu\text{J/pulse}$) and the generated ultraviolet pulse is used to excite the sample. The polarization directions of the various incoming pulses are controlled and adjusted by means of wave-plates and high quality Thomson–Glan prisms. The relative delays between the ω_{uv} , the ω_1 and the ω_2 pulses, focused into the sample by a 15 cm focal-length lens, are adjusted using optical delay lines with a resolution of 60 fs. The CARS signal, generated in a different direction from the incoming beams, is spatially filtered by an aperture, sent through a polarizer and focused on the slit of the spectrograph coupled to an OMA. The CARS spectra are recorded with and without UV excitation of the sample by accumulating 200 laser shots for a given time delay Δt_{exc} between the ω_{exc} pulse and with the ω_1 and ω_2 pulses in time coincidence. We were able to observe the evolution of the excited vibrational modes of the DNS molecule on a picosecond time-scale by using this procedure for different time delays Δt_{exc} , and it was therefore possible to follow the formation of the ICT state.

Before presenting the results, it is important to note that a strict comparison between the kinetics obtained from CARS signals and the kinetics obtained from “pump–probe” experiments is difficult. Indeed, when structural and stabilization processes occurs, not only may the population of a state change, but also parameters such as the electronic and vibrational oscillator strength of the bands associated to a same state. For example, the oscillator strength may change while the population stays the same. Also, the bond length may vary within a stable population. Consequent-

ly, kinetics must include different parameters which are not necessarily correlated to the population. Though the kinetics will belong to the same time scale whether studied using CARS results or using “pump–probe” results, they will probably not be strictly identical. In order to extract from the observed kinetics the true signal, exclusively due to the population evolution, difficult deconvolution procedures must be performed so as to discard changes due to structural and stabilization processes which also vary as a function of time inside a population which stays the same. It is important to recall these limitations before presenting the results we obtained.

Results and Discussion

Femtosecond Transient Absorption Experiments.

Pump-probe experiments were realized with DNS dissolved in nonpolar heptane, toluene, diethyl ether, and acetonitrile, in order to vary the polarity from nonpolar to strongly polar solvents. Ground state absorption and steady-state fluorescence spectra of DNS in heptane, toluene, diethylether, and acetonitrile solutions at room temperature are shown in Fig. 2. The ground state absorption spectrum of DNS, described in Fig. 2a, shows a strong $S_0 \rightarrow S_1$ absorption band located at 428 nm in the toluene solution, the band being slightly red-shifted (< 20 nm) for solvents of higher polarity.^{5,10} Therefore, the excitation wavelength at 400 nm used in our experiments populates the first excited state called E^* .⁵

Fig. 2b, which shows the steady state emission spectra, reveals very different behaviors in non-polar, slightly polar and

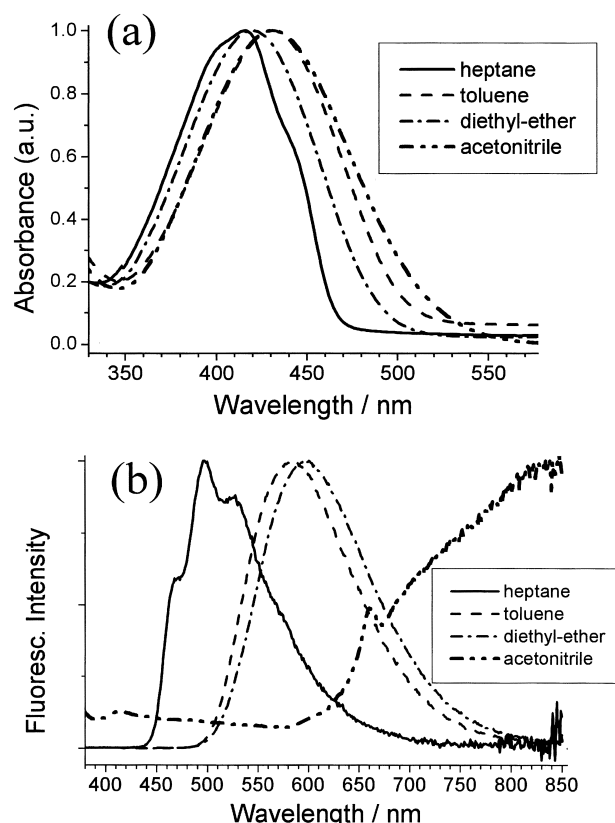


Fig. 2. Absorption (a) and fluorescence (b) spectra of DNS in heptane, diethyl ether, toluene, and acetonitrile.

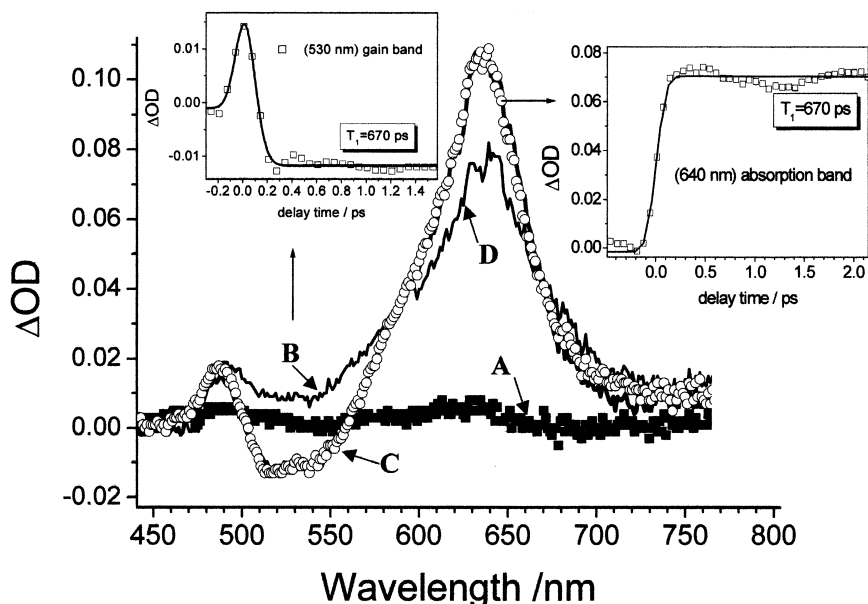


Fig. 3. Transient absorption spectra of DNS in heptane obtained for different delays Δt (A: -150 fs, B: 0 fs, C: 300 fs, D: 1.5 ps) after 400 nm excitation. Insets: Kinetics of the absorption (640 nm) and gain (530 nm) bands of excited DNS as a function of pump pulse delay.

strongly polar solvents. While a red shift of the emission spectrum of the order of 3000 cm^{-1} is observed in moderately polar solvents, revealing a strong charge transfer state stabilized by solvent interactions, very large and unexpected shifts are observed in highly polarized solvents, as for example in acetonitrile, while at the same time the emission intensity strongly decreases. As already mentioned,¹⁴ this indicates a change of the photophysical behavior of the compound for highly polar solvents.

These preliminary experiments are well correlated to the “pump–probe” transient absorption experiments shown in Figs. 3–6.

In the non-polar solvent *n*-heptane a very simple behavior is observed. As shown in Fig. 3, we observe a gain band at 530 nm and an absorption band at 630 nm, which appear immediately and then decreases with a lifetime of 670 ps. Some evolution of the band shape may be observed, but this can be explained if we suppose that the single excited state populated just after excitation also has some vibrational relaxation.

In the slightly polar solvent diethylether and the slightly interacting solvent toluene, the observations are different. While at short time delays, just after excitation, the transient spectra look the same as in *n*-heptane with the presence of the (slightly shifted) gain and absorption bands, respectively, in the 520 – 560 nm and 600 – 640 nm range, for longer times, the situation is different. When increasing the time delays, the rise of a new gain band around 630 – 660 nm is clearly visible. At the same time, the absorption band in the 600 – 650 nm range changes; in toluene, for example, a shoulder appears (see Fig. 4a). These new bands, as compared to the behavior in *n*-heptane, are a clear demonstration that a new excited state is formed and stabilized in these two interacting solvents. The same kinetics (see Figs. 4b and 5b) are observed for the gain band and for the absorption band, showing that these bands belong to the same excited state. The measured kinetics are well reproduced

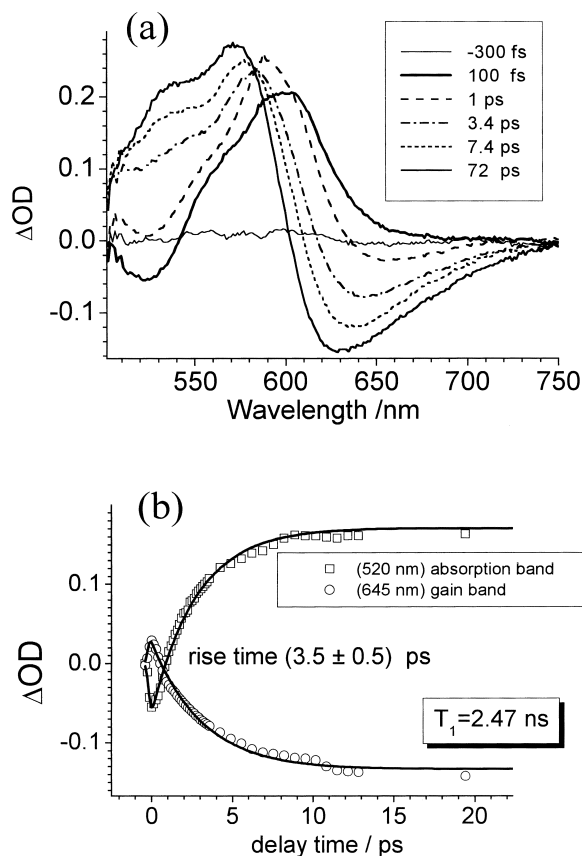


Fig. 4. (a): Transient absorption spectra of DNS in toluene. Spectra are obtained for different delays ($\Delta t = -300$ fs, 100 fs, 1 ps, 3.4 ps, 7.4 ps, 72 ps) after 400 nm excitation. (b): Kinetics of the absorption (520 nm) and gain (645 nm) bands of excited DNS as a function of pump pulse delay. A (3.5 ± 0.5) ps rise-time is obtained from the fits (solid curves).

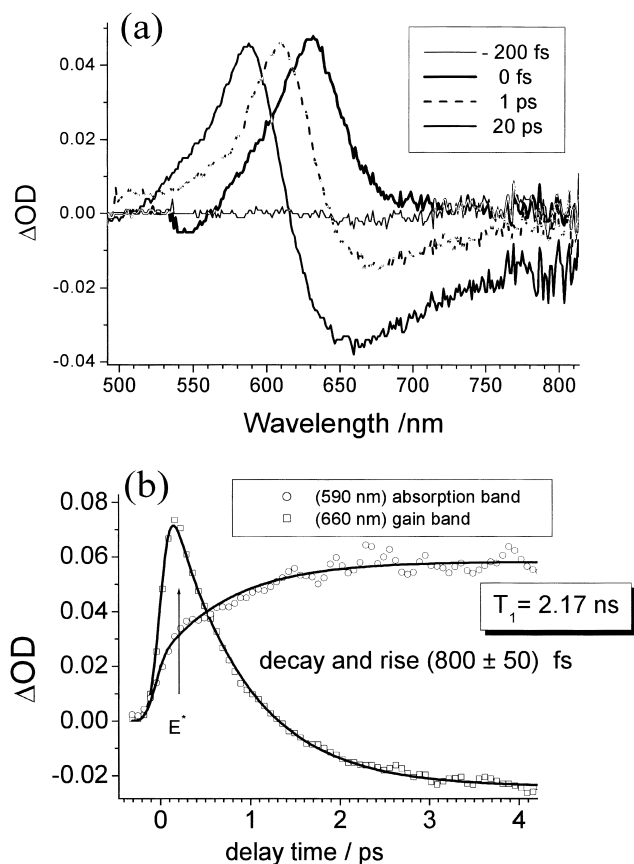


Fig. 5. (a): Transient absorption spectra of DNS in diethyl ether. Spectra are given at -200 fs, 0 fs, 1 ps, 20 ps delays after 400 nm excitation. (b): Kinetics of the absorption band (at 590 nm) and gain band (at 660 nm) of excited DNS as a function of pump pulse delay. A (800 ± 50) fs rise-time is obtained from the fits (solid curves).

(Figs. 4b and 5b) by the model of a two level system having a precursor-successor relationship.

To summarize, in these two solvents we observed the formation of a new state stabilized by interaction with the solvent. At this point, it is important to note that while diethyl ether is a slightly polar solvent ($\epsilon = 4.3$, $E_T(30) = 34.5$), indicating interactions due to polarity, toluene is not really a polar solvent ($\epsilon = 2.3$, $E_T(30) = 33.9$) but is polarizable due to the presence of aromatic rings. This means that the stabilization process is not limited to dipolar interactions but may also include other kinds of interaction forces. These observations are consistent with the assignment of the new state as an ICT state, called $A_{2,4}^*$ as explained in the introduction.

In highly polar acetonitrile ($\epsilon = 37.5$, $E_T(30) = 45.6$) the situation is again quite different from that observed in the last three solvents studied (see Fig. 6). At short time delays (the shortest possible times to be compatible with the experimental set-up), the transient spectra look the same as those in diethyl ether or toluene with a similar absorption band near 600 nm and a gain band in the far red (well correlated to the emission spectra). With increasing time delays, these bands evolve differently. In particular, a new absorption band appears around 520 nm, which has not been observed in the other solvents

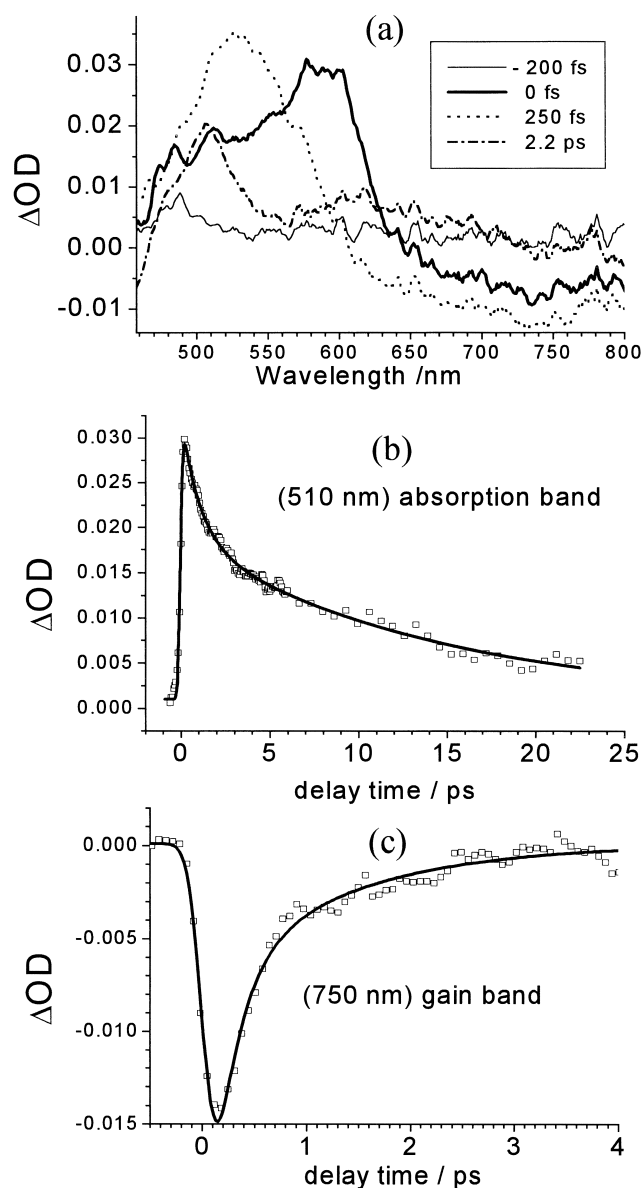


Fig. 6. (a): Transient absorption spectra of DNS in acetonitrile for -200 fs, 0 fs, 250 fs, 2.2 ps delay after pump excitation. (b): Kinetics of the absorption band at 510 nm as a function of pump pulse delay. A biexponential fit (solid curve) gives decay times $\tau_1 = (1.0 \pm 0.2)$ ps and $\tau_2 = (13 \pm 1)$ ps. (c): Kinetics of the gain band at 750 nm of excited DNS as a function of pump pulse delay. Decay times $\tau_1 = (300 \pm 50)$ fs and $\tau_2 = (1.2 \pm 0.2)$ ps are given by a biexponential fit.

studied. The kinetic of this new absorption presents a biexponential decay, well-fitted by the time constants $\tau_1 = (1.0 \pm 0.2)$ ps and $\tau_2 = (13 \pm 1)$ ps. As to the temporal behavior of the gain band, we notice a very fast decay with a time scale smaller than 2 ps. From these further observations, it is reasonable to attribute the decay of the absorption band to the non radiative relaxation of the $A_{2,4}^*$ state, whereas the fast decay of the gain band can be attributed to the relaxation of the ICT state called E^* which is formed just after excitation.

These results in different solvents show that, depending on

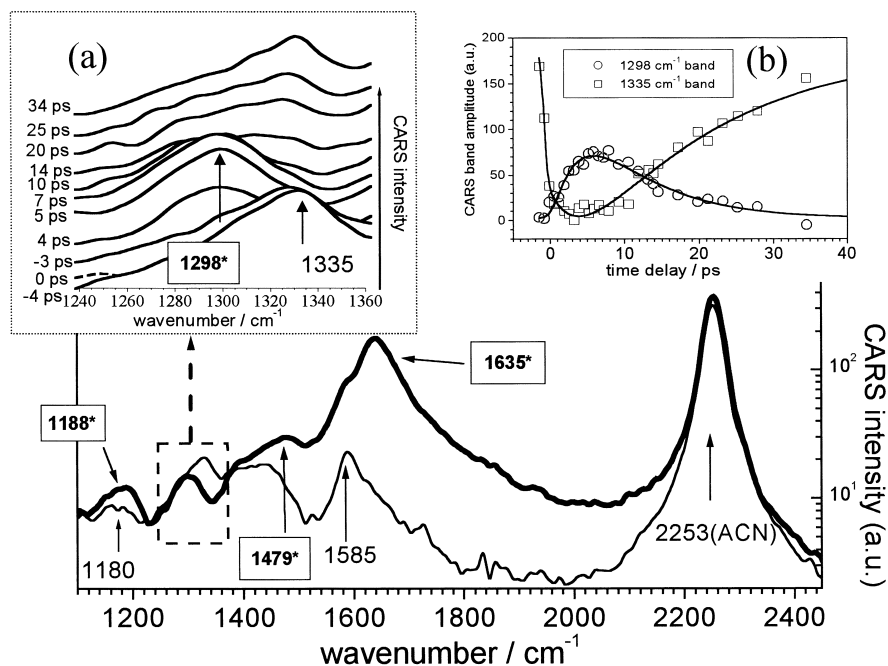


Fig. 7. Transient polarization sensitive CARS spectra of DNS in acetonitrile with ($\Delta t_{uv} = 5$ ps, (bold solid line)) and without UV excitation (thin solid line). Position of Raman bands of excited DNS are framed and indicated by an asterisk. Inset (a): Details of CARS spectra representing the NO_2 symmetric stretching mode bands of the S_1 excited state (1298 cm^{-1}) and the S_0 ground state (1335 cm^{-1}) of DNS in acetonitrile for different delays (Δt_{uv}) after UV excitation. Inset (b): Evolution of the amplitude of the excited state band (at 1298 cm^{-1}) and ground state band (at 1335 cm^{-1}) of DNS in acetonitrile as a function of UV pulse delay (Δt_{uv}).

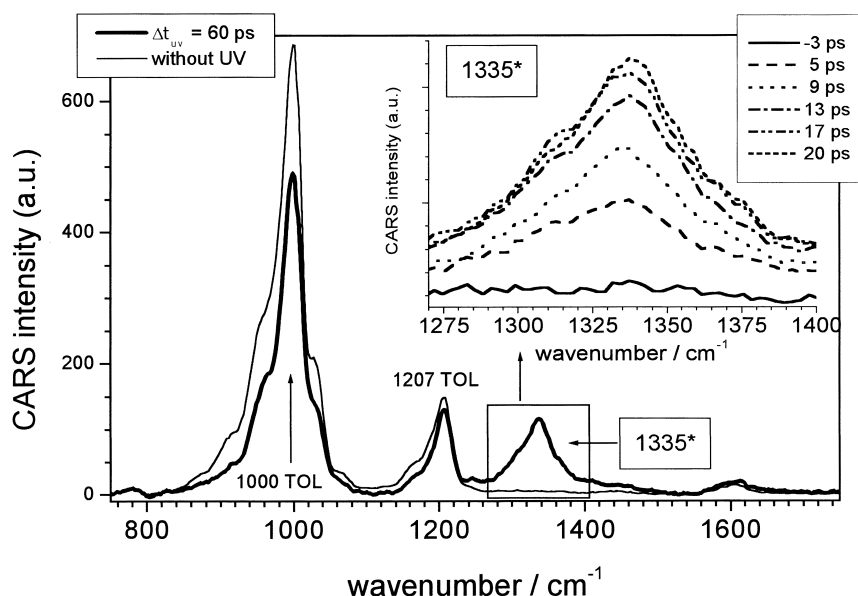


Fig. 8. Transient polarization sensitive CARS spectra of DNS in toluene with (bold solid line) and without UV excitation (thin solid line). Inset: 1335 cm^{-1} band of excited DNS in toluene for different delays (Δt_{uv}) after UV excitation at 300 nm.

the strength of the interaction with the solvent, two different excited states are formed and stabilized. According to the scheme proposed in Ref. 5 and involving the so-called $A_{2,4}^*$ and A_5^* states (see the introduction mentioned above), it is natural to assign the final stabilized state to the $A_{2,4}^*$ state in diethyl ether and toluene, and to the A_5^* state in acetonitrile.

Picosecond Time-Resolved CARS Experiments. It is

worth noting that these assignments are well supported by previous results¹⁴ obtained by the CARS experiments summarized in Figs. 7 and 8.

As already explained, the formation and stabilization of state A_5^* imply the formation of a charge transfer state mainly involving the strong acceptor character of the NO_2 group. Results shown in Fig. 7 (DNS in acetonitrile) show a strong evo-

lution of the symmetric stretch mode of NO₂ at 1335 cm⁻¹ which is downshifted by 37 cm⁻¹ after excitation. On the other hand, in solvents such as toluene, such a vibrational evolution is not observed, a result which agrees with the expected charge transfer character of the A^{*}_{2,4} state, in which the role of the NO₂ group is minimal, since the charge delocalization is mainly driven by the dimethylamino group.

This comparison proves that both CARS and "pump-probe" experiments are in good agreement with the same kinetic model explaining the photophysics of the DNS molecule.

Conclusion

In this paper, time-resolved transient absorption studies of DNS have revealed different behaviors as a function of solvent interactions. These results correlate well with the time-resolved CARS experiments published previously. For the first time, to our knowledge, two kinds of already predicted excited states are clearly identified. We have also observed their kinetic evolutions, which should give information about the different formation pathways of these states. These kinetics also strongly depend on the interactions with the solvent. Complicated behaviors occur which require a reconciliation between the different results obtained by "pump-probe" and by CARS experiments in different solvents. However, this lies beyond the scope of this paper and will be the object of a forthcoming publication.

References

- 1 W. R. Rettig, W. Majenz, R. Lapouyade, and M. Vogel, *J. Photochem. Photobiol., A*, **65**, 95 (1992).
- 2 W. R. Rettig, W. Majenz, and R. Lapouyade, *J. Photochem. Photobiol., A*, **62**, 415 (1992).
- 3 E. Gilabert, R. Lapouyade, and C. Rullière, *Chem. Phys. Lett.*, **145**, 262 (1988).
- 4 R. Lapouyade, K. Czeschka, W. Majenz, W. Rettig, E. Gilabert, and C. Rullière, *J. Phys. Chem.*, **96**, 9643 (1992).
- 5 R. Lapouyade, A. Kuhn, J. F. Letard, and W. Rettig, *Chem. Phys. Lett.*, **208**, 48 (1993).
- 6 N. Eilers-König, T. Kühne, D. Schwarzer, P. Vöhringer, and J. Schroeder, *Chem. Phys. Lett.*, **253**, 69 (1996).
- 7 Y. V. Il'ichev and K. A. Zachariasse, *Ber. Bunsenges Phys. Chem.*, **101**, 625 (1997).
- 8 E. Abraham, J. Oberlé, G. Jonusauskas, R. Lapouyade, and C. Rullière, *Chem. Phys.*, **214**, 409 (1997).
- 9 H. Görner and D. Schulte-Frohlinde, *J. Mol. Structure*, **84**, 227 (1982).
- 10 H. Gruen and H. Görner, *J. Phys. Chem.*, **93**, 7144 (1989).
- 11 H. Görner, *Ber. Bunsen-Ges. Phys. Chem.*, **102**, 726 (1998).
- 12 M. Hashimoto and H. Hamaguchi, *J. Phys. Chem.*, **99**, 7875 (1995).
- 13 H. Okamoto and M. Tasumi, *Chem. Phys. Lett.*, **256**, 502 (1996).
- 14 J. Oberlé, E. Abraham, G. Jonusauskas, and C. Rullière, *J. Raman Spectrosc.*, **31**, 311 (2000).
- 15 G. Riezebos and E. Havinga, *Rec. Trav. Chim. Pays Bas*, **80**, 446 (1991).
- 16 G. Jonusauskas, J. Oberlé, and C. Rullière, *Opt. Lett.*, **23**, 1918 (1998).
- 17 G. Lucassen, "Polarization Sensitive Coherent Raman Spectroscopy on (Bio)Molecules in Solutions," Ph. D. Thesis, University of Twente, The Netherlands (1992), (INSB: 90-9005526-6).
- 18 A. Y. Chikishev, G. W. Lucassen, N. I. Koroteev, C. Otto, and J. Greve, *Biophys. J.*, **63**, 976 (1992).
- 19 R. J. H. Clark and R. E. Hester, "Time Resolved Spectroscopy, Advances in Spectroscopy," Vol. 15 (1989).
- 20 N. I. Koroteev, A. P. Shkurinov, and B. N. Toleutaev, in "Coherent Raman Spect. Recent Adv.," ed by G. Marowsky and V. V. Smirnov, Springer Proc. in Phys., Vol. 63, Springer-Verlag (1992), pp.186-204.
- 21 J. Oberlé, E. Abraham, A. Ivanov, G. Jonusauskas, and C. Rullière, *J. Phys. Chem.*, **100**, 10179 (1996).